

Neutron powder diffraction study of crystal and magnetic structures of orthorhombic LuMnO₃

H. Okamoto^a, N. Imamura^b, B.C. Hauback^c, M. Karppinen^{b,d}, H. Yamauchi^b, H. Fjellvåg^{a,*}

^a Centre for Materials Science and Nanotechnology, Department of Chemistry, University of Oslo, Blindern, NO-0315 Oslo, Norway

^b Materials and Structures Laboratory, Tokyo Institute of Technology, Yokohama 226-8503, Japan

^c Institute for Energy Technology, NO-2027 Kjeller, Norway

^d Laboratory of Inorganic and Analytical Chemistry, Helsinki University of Technology, FI-02015 TKK, Finland

Received 19 November 2007; received in revised form 21 January 2008; accepted 24 January 2008 by C. Lacroix

Available online 7 February 2008

Abstract

The crystal and magnetic structures of orthorhombic, perovskite-type LuMnO₃ are described on the basis of neutron powder diffraction data; space group *Pbnm*, $a = 5.19865(14)$ Å, $b = 5.78853(15)$ Å, and $c = 7.2970(2)$ Å at 298 K. There is a strong cooperative Jahn–Teller (JT) distortion of the MnO₆-octahedra resulting in orbital ordering and *E*-type antiferromagnetic order below $T_N \sim 40$ K. The magnetic propagation wave vector is commensurate $\mathbf{k} = \mathbf{b}^*/2$ at 8 K and no indications of any magnetic phase transitions are seen in susceptibility data. The ordered magnetic moment for Mn is $3.4 \mu_B$.

Published by Elsevier Ltd

PACS: 71.70.Ej; 75.25.+Z; 75.47.Lz; 75.50.Ee

Keywords: A. High-pressure synthesis; B. LuMnO₃; C. Crystal structure and symmetry; D. Magnetic property

The rare-earth manganese oxides, REMnO₃, have been the target of intensive research for the last decade, partly due to the observed colossal magnetoresistance (CMR) effect in e.g. La_{1-x}A_xMnO₃ [1,2]. Two different crystal structure types appear as functions of the radius of the RE element at ambient conditions; (i) the perovskite o-REMnO₃-type structure (orthorhombic; space group *Pbnm*) for RE = La–Dy and (ii) a non-centrosymmetric layer-like hexagonal h-REMnO₃ structure (space group *P6₃cm*) for RE = Ho–Lu, Y, and Sc [3,4]. The relative stability between the structure types appears to be dominated by the size effect of the RE element. In the orthomanganese perovskite-type oxides, the relative size of the 12-coordinated RE *versus* the 6-coordinated Mn is described in terms of a tolerance factor $t = d(\text{RE–O})/\sqrt{2}d(\text{Mn–O})$. A mismatch of the bond length between RE–O and Mn–O results in tilting of the rather

rigid MnO₆-octahedra and hence deviation of the Mn–O–Mn bond angles from 180°. For Mn^{III} being a *d*⁴ ion, a strong Jahn–Teller (JT) distortion is observed in these perovskite-type oxides, resulting in 4 short and 2 long Mn–O bond distances below the JT transition (T_{JT}). By resorting to high-pressure techniques, the more volume efficient perovskite modification is becoming stabilized also for RE = Ho–Lu. In addition to high-pressure synthesis techniques [5], low temperature soft chemistry [6], and epitaxial thin film growth [7] may also stabilize the perovskite modification.

The variation of selected crystal structure parameters for orthomanganese o-RE³⁺MnO₃ oxides, is visualized as a function of RE³⁺ ionic radius in Fig. 1. While the *a*- and *c*-axes and the unit-cell volume decrease monotonically with decreasing ionic radius, the *b*-axis remains essentially unchanged. The size of the JT distortion in terms of $d(\text{Mn–O})$ bond distances is seen to remain fairly constant. For large REs [8], an *A*-type antiferromagnetic (AFM) ordering takes place at low temperatures. Here the spin moments are coupled ferromagnetically in the *ab-plane* and antiferromagnetically along the *c*-axis. This ordering involves an ordered pattern of

* Corresponding address: Centre for Materials Science and Nanotechnology, Department of Chemistry, University of Oslo, P.O. Box 1033 Blindern, NO-0315 Oslo, Norway. Tel.: +47 22 85 55 64; fax: +47 22 85 54 41.

E-mail address: helmer.fjellvag@kjemi.uio.no (H. Fjellvåg).

$d_{3x^2-z^2}$ [long d (Mn–O)] and $d_{x^2-y^2}$ orbitals [short d (Mn–O)]. For RE = Tb, Dy, and Ho the magnetic ground state is an AFM spiral structure [9]. Upon further decreasing the ionic radius, the ground state of the magnetic structure changes to E -type AFM for o-YbMnO₃ [10]. Muñoz et al. in Ref. [11] discussed the different magnetic ground states between the larger (e.g. LaMnO₃) and smaller (e.g. o-HoMnO₃) RE-oxides in terms of the Goodenough–Kanamori rule [12]. The enhanced tilting of the octahedra weakens the superexchange interactions between the nearest neighbors, and hence increasing the importance of next-nearest-neighbor interactions. Brinks et al. showed in Ref. [13] that the propagation wave vector k of the incommensurate structure varies with the size of the RE³⁺. Kimura et al. [14] investigated the magnetic properties of this HoMnO₃ and suggested the presence of a frustrated spin system with ferromagnetic (FM) nearest-neighbor and AFM next-nearest-neighbor interactions within MnO₂ planes with basis on microscopic calculations. This model was later supported by heat capacity measurements of Tachibana et al. for RE = Ho–Lu [15]. On the other hand, Zhou and Goodenough [16] claimed that the so far reported constant T_N ordering temperature in E -type o-REMnO₃ oxides is connected with the distortions of the octahedra (cf. the Mn–O2–Mn separations in Fig. 1; *i.e.* the longest (l) and shortest bond (s) distances) and not to the variation in bond angles, and that this also holds for the competition of FM e_g –O– e_g and AFM t_{2g} –O– t_{2g} interactions. One reason for this controversy is probably the lack of structural parameters for the o-REMnO₃ oxides with small REs.

We have previously reported on the successfully synthesis of o-LuMnO₃ by means of an ultra-high-pressure technique [17] as well as on its magnetic and electric properties. o-LuMnO₃ undergoes an antiferromagnetic transition at $T_N \sim 40$ K. Insulating behaviour with negative gradient of $\delta\rho/\delta T$ is observed below 400 K. These behaviors are similar to those for other isostructural o-REMnO₃. Presently we provide crystal and magnetic structure data for LuMnO₃, as determined from high-resolution neutron powder diffraction measurements, and discuss the observed E -type AFM structure and strong cooperative JT distortion in relation to other o-REMnO₃ phases.

Polycrystalline, single phase samples of o-LuMnO₃ were prepared in a cubic-anvil-type high-pressure apparatus at 5 GPa maintained at 800 °C for 30 min. The details are given in Ref. [17]. Neutron powder diffraction (NPD) data were collected at 298 K and 8 K with the PUS two-axis high-resolution diffractometer at the JEEP II reactor, Kjeller, Norway [18]. Cylindrical vanadium sample holders were used. Monochromatized neutrons of wavelength 1.5554 Å were obtained by reflection from Ge (311). Diffraction data were measured in the range $10.00^\circ \leq 2\theta \leq 129.95^\circ$ and rebinned into 2400 datapoints in steps of $\Delta 2\theta = 0.05^\circ$. All refinements were performed with the Fullprof code [19] according to the Rietveld method [20]. The Thompson–Cox–Hastings pseudo-Voigt profile shape function was adopted. The background was described by linear interpolation between selected points. Isotropic displacement parameters were refined for the different

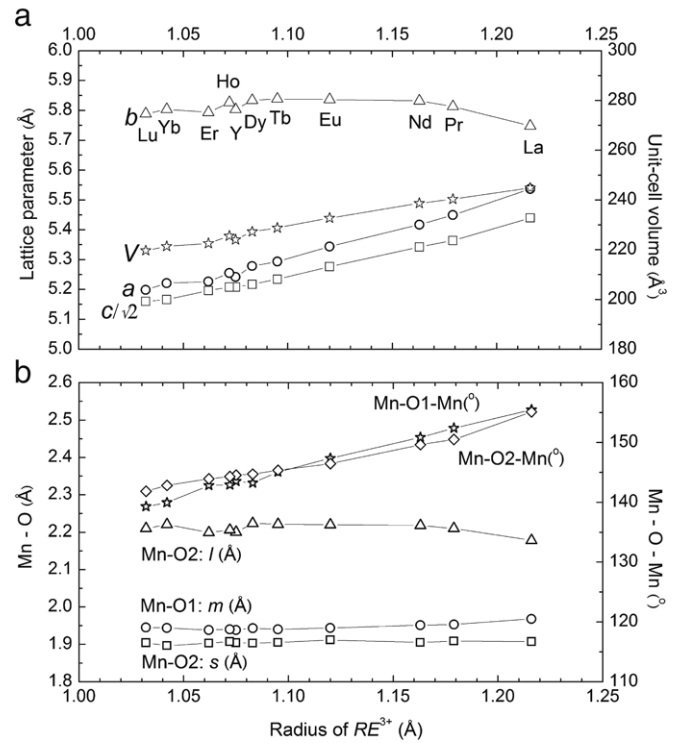


Fig. 1. The variation of (a) unit-cell parameters (left axis) and unit-cell volume (right axis) of o-REMnO₃, (b) bond distances (left axis) and bond angles (right axis) between Mn and O as functions of RE³⁺. Data for RE = Lu (present work); for RE = La–Er taken from Ref. [8], except for Eu, Ho, and Yb taken from Refs. [24,13,10] respectively.

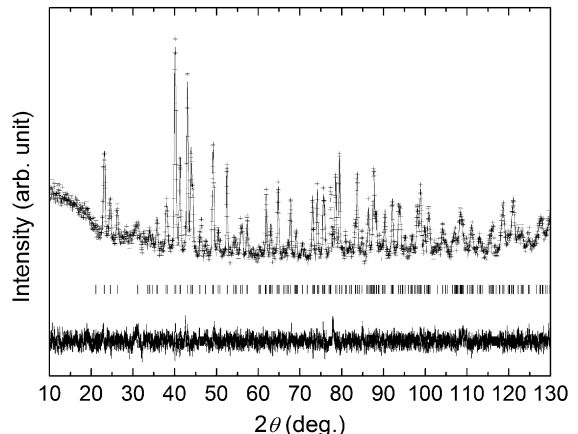


Fig. 2. NPD pattern of LuMnO₃ at 298 K. Observed (+), calculated (solid line) and difference intensity profiles according to Rietveld refinement; Bragg positions shown as vertical bars.

types of atoms of Lu, Mn, and O. Reflections from the Displex cryostat at $46.00^\circ \leq 2\theta \leq 46.90^\circ$, $76.90^\circ \leq 2\theta \leq 77.60^\circ$, and $115.90^\circ \leq 2\theta \leq 117.20^\circ$ were excluded prior to the refinements.

The crystal structure of LuMnO₃ was determined at 298 K from NPD data, space group $Pbnm$; $a = 5.19865(14)$ Å, $b = 5.78853(15)$ Å, and $c = 7.2970(2)$ Å. The final fit obtained from the Rietveld refinement is shown in Fig. 2.

Table 1

Crystallographic data from Rietveld refinement of neutron powder diffraction data for LuMnO₃, space group *Pbnm*

(A)		
LuMnO ₃	298 K	8 K
<i>a</i> (Å)	5.19865(14)	5.18958(10)
<i>b</i> (Å)	5.78853(15)	5.78498(11)
<i>c</i> (Å)	7.2970(2)	7.28150(16)
Volume (Å ³)	219.587(18)	218.602(13)
<i>R</i> _p	3.46	4.59
<i>R</i> _{wp}	4.42	5.88
<i>R</i> _{exp}	4.64	5.24
χ^2	0.907	1.26

(B)			
Atom	Wyckoff position/Isotropic displacement parameter ^a	298 K	8 K
Lu	4c(<i>x y</i> 1/4)		
	<i>x</i>	0.5182(7)	0.5191(7)
	<i>y</i>	0.5849(5)	0.5874(5)
	<i>B</i> (Å ²)	0.20(5)	0.17(5)
Mn	4b (1/2 0 0)		
	<i>B</i> (Å ²)	0.34(11)	0.44(10)
O1	4c (<i>x y</i> 1/4)		
	<i>x</i>	0.3790(7)	0.3787(8)
	<i>y</i>	−0.0431(7)	−0.0422(7)
	<i>B</i> (Å ²) ^a	0.17(3)	0.32(4)
O2	8d (<i>xyz</i>)		
	<i>x</i>	0.6958(5)	0.6978(5)
	<i>y</i>	0.3311(5)	0.3297(5)
	<i>z</i>	0.0570(4)	0.0576(4)
	<i>B</i> (Å ²) ^a	0.17(3)	0.32(4)

Calculated standard deviations in parentheses. (A) Unit-cell dimensions, and figure of merit. (B) Atomic coordinates, displacement parameters.

^a Constrained to the same values for O1 and O2.

Refined structural parameters are listed in Table 1, while bond lengths and bond angles are listed in Table 2. The bond lengths clearly indicate the presence of a strong JT distortion; two longer bonds of 2.210(3) Å and two sets of shorter distances, *i.e.* 1.9457(13) Å and 1.904(3) Å. These data correspond to a polyhedron-distortion parameter [21] $\Delta = 45.0(2) \times 10^{-4}$ for the octahedrally-coordinated Mn. The distortion parameter is significantly larger than that found for LaMnO₃ (33.1×10^{-4} at 300 K [8]). A review of structure data for various o-REMnO₃ show unsystematic scatter in Δ for the heavier RE, yet all with a Δ considerably larger than that for LaMnO₃. The calculated bond angles of 139.3(2)° and 141.84(15)° between Mn and O are consistent with a large tilting of the octahedra.

A close inspection of the NPD pattern at 8 K, see Fig. 3, reveals additional magnetic reflections that are not consistent with the nuclear unit cell. The magnetic reflections were indexed on the cell $a = 5.18958(10)$ Å, $b = 5.78498(11)$ Å, and $c = 7.28150(16)$ Å, with a propagation wave vector of $\mathbf{k} = \mathbf{b}^*/2$. No satellite peaks that could indicate an incommensurate magnetic structure were observed. The strong magnetic reflection of (0 1/2 0) at $d \sim 3.8$ Å clearly proves the doubling of the *b*-axis. The manganese atoms (Mn1

Table 2

Calculated bond distances, bond angles, bond-valence sum (B.V.S.) and JT-distortion parameter (Δ) for REMnO₃ with RE = Lu (present data) and RE = La (Ref. [8]) included in [] for comparison

LuMnO ₃	298 K	8 K
Lu–O1 (Å)	3.219(5) [3.158(2)]	3.213(6)
Lu–O1 (Å)	2.271(5) [2.560(2)]	2.262(5)
Lu–O1 (Å)	2.194(5) [2.425(2)]	2.197(6)
Lu–O2 (Å) $\times 2$	2.548(3) [2.698(2)]	2.552(3)
Lu–O2 (Å) $\times 2$	2.494(4) [2.650(2)]	2.466(4)
Lu–O2 (Å) $\times 2$	2.234(4) [2.459(2)]	2.246(4)
$\langle \text{Lu–O} \rangle$ (Å)	2.471(4) [2.639(2)]	2.467(4)
B.V.S. (CN = 9) ^a	2.91(3)	2.92(3)
Mn–O1 (Å) $\times 2$ (<i>m</i>)	1.9457(13) [1.9680(3)]	1.9414(14)
Mn–O2 (Å) $\times 2$ (<i>s</i>)	1.904(3) [1.907(1)]	1.899(3)
Mn–O2 (Å) $\times 2$ (<i>l</i>)	2.210(3) [2.178(1)]	2.206(3)
$\langle \text{Mn–O} \rangle$ (Å)	2.020(2) [2.0178(4)]	2.015(2)
Δ (Mn–O) $\times 10^{-4}$ ^b	45.0(2) [33.1]	45.48(18)
B.V.S. (CN = 6) ^a	3.156(16)	3.197(19)
Mn–O1–Mn (°) $\times 2$	139.3(2)	139.3(2)
Mn–O2–Mn (°) $\times 4$	141.84(15)	142.24(15)
$\langle \text{Mn–O–Mn} \rangle$ (°)	140.99(17) [155.23(3)]	141.226(17)

^a Adopted bond-valence parameters of Lu³⁺–O^{2−} and Mn³⁺–O^{2−} are 1.971 and 1.76, respectively [23].

^b The distortion parameter of Δ for MO_N polyhedron with an average M–O distance of $\langle \text{M–O} \rangle$, is defined as $\Delta = (1/N) \sum_{n=1,N} \{(\text{M–O}) - (\text{M–O})\} / \langle \text{M–O} \rangle^2$.

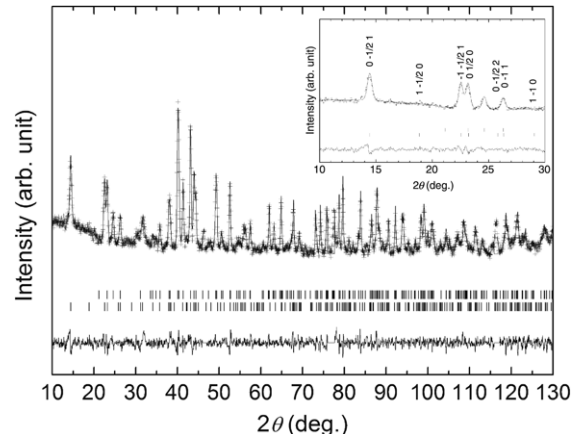


Fig. 3. NPD pattern of LuMnO₃ at 8 K. Observed (+), calculated (solid line) and difference intensity profiles according to Rietveld refinement; Bragg positions of nuclear (upper) and magnetic (lower) reflections shown as vertical bars. Inset shows a selected 2θ region with indexes for magnetic reflections.

to Mn4) occupy the 4b Wyckoff position; *i.e.* (1/2, 0, 0), (1/2, 0, 1/2), (0, 1/2, 0), and (0, 1/2, 1/2). The possible irreducible magnetic representations for $\mathbf{k} = \mathbf{b}^*/2$ in space group *Pbnm* are $\Gamma = 3\Gamma_1 + 3\Gamma_2$ according to Kovalev's notation [22]. Further details on the symmetry analysis for orthomanganese oxides are given by Brinks et al. [13]. The best fit for the experimental NPD data at 8 K was obtained for the basis function corresponding to the Γ_1 representation. In this *E*-type collinear antiferromagnetic structure (see Fig. 4(b)) the ordered Mn moments are antiferromagnetically aligned along the *b*- and *c*-axes. The refined magnetic moment is

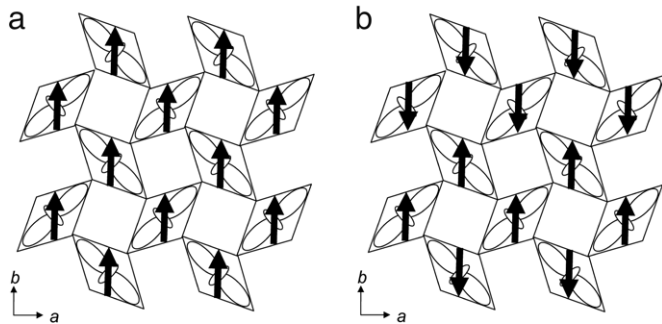


Fig. 4. Schematic representations of the (a) A-type and (b) E-type magnetic structures occurring for REMnO_3 .

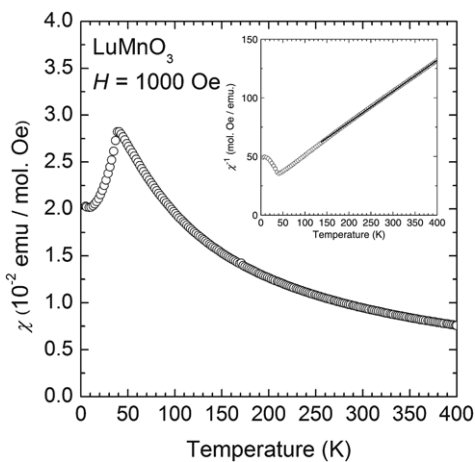


Fig. 5. Magnetic susceptibility measured in field of 1000 Oe as function of temperature for LuMnO_3 . The inset shows inverse susceptibility and fit according to the Curie–Weiss law.

$\mu_{\text{AF}}(\text{Mn}) = 3.37(4) \mu_B$ (see Table 3). It is worth adding that mixing of other basis vectors with a - and c -axes components in the IR Γ_1 will lead to canted structures. However, none of these gave any improved fit in the refinements. No indications of a ferromagnetic component was found in the magnetization data (*vide infra*) and non-collinear models were hence excluded. The refined magnetic moment of $3.37(4) \mu_B$ is to be compared with e.g. $3.96 \mu_B$ for HoMnO_3 [13] and $3.45(5) \mu_B$ for YbMnO_3 [10].

The present investigation confirms that LuMnO_3 takes the E-type magnetic structure as suggested on the basis of consideration of exchange interactions [14,15], and hence confirms that commensurate AFM occurs for both YbMnO_3 and LuMnO_3 . This supplements the magnetic phase diagram for REMnO_3 with A-type AFM for the larger REs, incommensurate order for Gd–Ho [13,14], and E-type for the smaller REs.

The temperature dependence of the magnetic susceptibility, χ , shows a sharp decrease at the onset of long range AFM ordering at the Néel temperature of $T_N \sim 40$ K, see Fig. 5. Above T_N , the susceptibility follows the Curie–Weiss law. The fitting of the data to $\chi = C/(T - \theta)$, yields an effective moment of $\mu_{\text{eff}} = 5.49 \mu_B$ and a negative Weiss temperature of $\theta = -98.3$ K. There is no deviation from the linear trend at temperatures above but still close

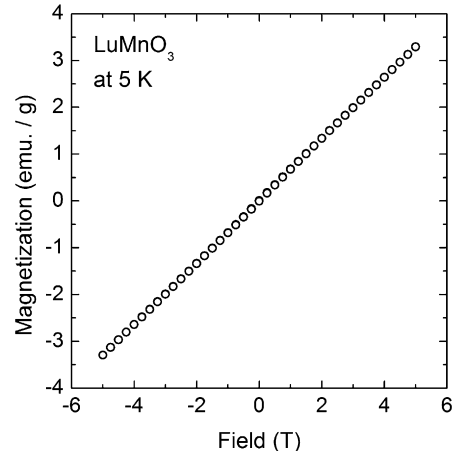


Fig. 6. Field dependence of the magnetization at 5 K for LuMnO_3 .

Table 3

Magnetic moment (m_x m_y m_z) of E-type antiferromagnetically ordered Mn at $4b$ site within the irreducible representation Γ_1 as determined from Rietveld refinements of NPD data at 8 K; figure of merits, R_{mag} and χ^2

IR	Γ_1
Magnetic moment (μ_B)	
m_x	0
m_y	3.37(4)
m_z	0
χ^2	1.26
R_{mag}	6.35

to T_N . The present dc- and ac-excited magnetization shows no indication of any magnetic transition that could suggest a temperature interval with incommensurate magnetic structure. The calculated effective paramagnetic moment corresponds to a spin-only value of $S = 2.29$, somewhat higher than that expected for Mn^{III} , and considerably higher than the observed ordered magnetic moment by NPD, $\mu_{\text{AF}} = 3.37(4) \mu_B$. This discrepancy may e.g. be due to deduction of μ_{eff} in a too low temperature regime, or to non-ideal paramagnetism owing to spin correlations etc. The dependence of the magnetization on magnetic field at 5 K for LuMnO_3 is shown in Fig. 6. A linear behavior was observed in accordance with a stable AFM ordered structure.

Orthorhombic LuMnO_3 with perovskite-type structure is synthesized by high-pressure methods. The crystal structure of this metastable polymorph of LuMnO_3 is investigated by powder neutron diffraction at ambient pressure and it shows a strong Jahn–Teller distortion. The Mn-atoms order antiferromagnetically in an E-type structure at 10 K. The Néel temperature is $T_N \sim 40$ K.

Acknowledgements

This work was supported by the Research Council of Norway, Grant. No. 158518/431 (NANOMAT), Grants-in-aid for Scientific Research (Nos. 15206002) from the Japan Society for the Promotion of Science, and Academy of Finland (Decision Nos. 114517 and 1162545).

References

- [1] R. Von Helmolt, J. Wecker, B. Holzapfel, L. Schultz, K. Samwer, Phys. Rev. Lett. 71 (1993) 2331.
- [2] H.Y. Hwang, S.-W. Cheong, P.G. Radaelli, M. Marezio, B. Batlogg, Phys. Rev. Lett. 75 (1995) 914.
- [3] H.L. Yakel, Acta Crystallogr. 9 (1955) 394.
- [4] H.L. Yakel, W.C. Koehler, F. Bertaut, E. Forrat, Acta Cryst. 16 (1963) 957.
- [5] A. Waintal, J.J. Capponi, E.F. Bertaut, M. Contré, D. Francois, Solid State Commun. 4 (1966) 125;
A. Waintal, J. Chevanas, Mater. Res. Bull. 2 (1967) 819.
- [6] S. Quezel, J.R. Mignod, E.F. Bertaut, Solid State Commun. 14 (1974) 941.
- [7] P.A. Salvador, T.-D. Doan, B. Mercey, B. Raveau, Chem. Mater. 10 (1998) 2592.
- [8] J.A. Alonso, M.J. Martínez-Lope, M.T. Casasis, Inorg. Chem. 39 (2000) 917.
- [9] T. Arima, A. Tokunaga, T. Goto, H. Kimura, Y. Noda, Y. Tokura, Phys. Rev. Lett. 96 (2006) 097202.
- [10] Y.H. Huang, H. Fjellvåg, M. Karppinen, B.C. Hauback, H. Yamauchi, J.B. Goodenough, Chem. Mater. 18 (2006) 2130;
Y.H. Huang, H. Fjellvåg, M. Karppinen, B.C. Hauback, H. Yamauchi, J.B. Goodenough, Chem. Mater. 19 (2007) 2139. (erratum).
- [11] A. Muñoz, M.T. Casáis, J.A. Alonso, M.J. Martínez-Lope, J.L. Martínez, M.T. Fernández-Díaz, Inorg. Chem. 40 (2001) 1020.
- [12] J.B. Goodenough, Magnetism and the Chemical Bond, Wiley, New York, 1963.
- [13] H.W. Brinks, J. Rodríguez-Carvajal, H. Fjellvåg, A. Kjekshus, B.C. Hauback, Phys. Rev. B 63 (2001) 094411.
- [14] T. Kimura, S. Ishihara, H. Shintani, T. Arima, K.T. Takahashi, K. Ishizaka, Y. Tokura, Phys. Rev. B 68 (2003) 060403.
- [15] M. Tachibana, T. Shimoyama, H. Kawaji, T. Atake, E. Takayama-Muromachi, Phys. Rev. B 75 (2007) 144425.
- [16] J.-S. Zhou, J.B. Goodenough, Phys. Rev. Lett. 96 (2006) 247202.
- [17] N. Imamura, M. Karppinen, H. Fjellvåg, H. Yamauchi, Solid State Commun. 140 (2006) 386.
- [18] B.C. Hauback, H. Fjellvåg, O. Steinsoll, K. Johansson, O.T. Buset, J. Jorgensen, J. Neutron Res. 8 (2000) 215.
- [19] J. Rodríguez-Carvajal, Physica B 192 (1993) 55.
- [20] H.M. Rietveld, J. Appl. Crystallogr. 2 (1969) 65.
- [21] R.D. Shannon, Acta Crystallogr. Ser. A 32 (1976) 751.
- [22] O.V. Kovalev, Irreducible Representation of Space Groups, Gordon and Breach, New York, 1985.
- [23] N.E. Brese, M. O'Keeffe, Acta Crystallogr. Ser. B 47 (1991) 192.
- [24] B. Dabrowski, S. Kolesnik, A. Baszcuk, O. Chmaissem, T. Maxwell, J. Mais, J. Solid State Chem. 178 (2005) 629.